The Noise Effects on Signal Processors Used for Fault Detection Purpose

Hossein Ehya*, Tarjei Nesbø Skreien*, Arne Nysveen*, and Robert Nilssen*

* Department of Electrical Power Engineering, Norwegian University of Science and Technology, 7030 Trondheim, Norway

Abstract—**Signal Processing plays a crucial role in addressing failures in electrical machines. Experimental data are never perfect due to the intrusion of undesirable fluctuations unrelated to the investigated phenomenon, so-called noise. Noise has disturbing effects on the measurement data, and in the same way, could diminish or mask the fault patterns in feature extraction using different signal processors. In this paper, fault detection in a custom made 100 *kVA* synchronous generator under an inter-turn short circuit fault is studied by using measurements of the air gap magnetic field. Signal processing tools like a Fast Fourier Transform (FFT), Short Time Fourier Transform (STFT), Discrete Wavelet Transform (DWT), Continuous Wavelet Transform (CWT), and Time Series Data Mining (TSDM) are used to diagnose the faults with a central focus on noise impacts on processed data. Moreover, some useful methods are presented for hardware noise rejection.**

Index Terms— **Fault diagnosis, noise, salient pole synchronous generator, signal processing.**

I. INTRODUCTION

Early-stage diagnosis of incipient faults in electrical machines can limit the progressive damages that lead to colossal economic losses. Over the past two decades, there has been a sustained research activity in the field of fault detection of electrical machines. Different approaches based on various signals that are acquired based on invasive methods like air-gap magnetic field monitoring or non-invasive methods as stator current, voltage, and torque are proposed to discriminate the fault.

Faults in electrical machines could be divided into three categories: electrical failures like short circuit fault of stator or rotor windings, or mechanical failures like static or dynamic eccentricity, broken damper bars, broken end ring, and misalignment. The demagnetization of permanent magnets is also classified as a magnetic fault in permanent magnetic machines. Each kind of failure could give rise to a specific symptom in the electrical machine, which may be observed in a measured signal [1].

Feature extraction and signal processing is the central part of a fault detection procedure. Numerous indices are proposed based on various signal processing tools to detect different types of faults in the electrical machines. However, the majority of results are based on a laboratory test rig or finite element simulation results, which do not consider the noise effect. However, some attempts have been made to address this issue in [2].

The working environment of electrical machines in the industries and power plants are susceptible to various kinds of noise that may have considerable consequences on measured signals [3]. The working environment of synchronous generators in hydropower plants is vulnerable to noise emitted from power transformers [4], the turbine, and the machine itself. Besides, the utilized induction motors in industries controlled by inverter drives may create interfering noise [5-7]. The amplitude and frequency of the emitted noise by inverters depend on the modulation techniques utilized in the power converters [7].

It has been reported in [8] that most of the varied industries are subjected to a high degree of complex noise which is the combination of white Gaussian noise with impulsive noise. The amplitude of the noise in the working environment of the industry depends on various criteria [9] and the noise profile varies from case to case. In addition to noise emitted from the equipment utilized in industry, faulty electric machines also cause some degree of noise [10], and the noise level is increased by increasing the fault severity.

The fault detection is based on the acquired signals from the faulty machine. If the working environment is vulnerable to noise, it is almost unavoidable that the signal is not contaminated by noise. Therefore, the effect of noise on the processed signals must be considered. In addition, the noise effect may cause indices found by feature extraction to give false fault identifications. Various signal processing tools utilized for condition monitoring systems respond to noise diversely. In this paper, several types of noise are introduced, and their effects on measured signals are investigated. Also, the effects of noise on signal processing tools like FFT, STFT, CWT, DWT, and TSDM are investigated. Furthermore, proposed indices for inter-turn short circuit detection of salient pole synchronous generator operating in a noisy environment are studied, and noise effect on results is discussed. Moreover, it is demonstrated that a certain level of noise, indices, and signal processing tools may work ineffectively. The utilized signal is acquired in a laboratory with various electric equipment that may contribute to noise interference of the signal under healthy and faulty conditions.

II. Signal and Noise

A. Definition

The term 'signal' in the field of condition monitoring means only desirable data that are measured. However, signals are vulnerable to noise during the process of acquisition, storage, or conversion. Noise is an unwanted signal that may disrupt the quality of the main signal. Every device in the power plant or industry that works based on electromagnetic law may be a noise source. The generated noise by each electric device has its own unique characteristics that fall into a specific category of noise. In order to quantify the quality of the signal, the signal-to-noise (S/N) ratio is expressed. It represents the ratio of the signal amplitude to the standard deviation of the noise [3].

B. Source of Noise in Industries

The radiated noise from electric equipment is generally limited to a discrete low-frequency signal. However, the electric machine, whether stationary like transformers or rotating machineries like electric motors or generators, generates a broadband noise component due to their cooling systems. The net noise is superimposed of the electromagnetic and cooling system components. Moreover, in variable speed drives, the power electronic converters that are frequently used in industries are an additional source of noise.

The noise in an electric machine is as below [3, 6]:

1. The electromagnetic source of noise in the electric machine is due to the radial force created by the interaction of the stator and rotor magnetic field. The structure of the rotor and the slot harmonics cause high-frequency components that in turn lead to force and noise inside the machine.
2. Aerodynamic source of noise has a broad frequency band that is generated due to the flow of the air at the inlet or outlet of the machine cooling system.
3. Mechanical source of noise is due to the natural frequency of the stator, improper installation of the machine, and bearing vibration. If the exciting frequency of the machine coincides with stator natural frequency, a strong noise will be created.

The amount of noise created by transformers is significant in comparison to rotating electric machines. The source of the noise in power transformers is divided into magnetic noise which is due to the magnetic field of the core and the load noise which is caused due to interaction of the leakage flux and the current passing through the coils [4]. However, the metallic body of the transformer may shield the emitted noise to the working environment, albeit the generated noise is unavoidable. Moreover, the power transformers in power plants are placed in a separate room that reduces their effect on the measuring parameter of the synchronous generator.

Many electrical motors use solid-state inverter drives to feed into windings. The power supply is not entirely sinusoidal and contains numerous harmonics. The most important harmonics created are 5th, 7th, and 11th, which become critical if mentioned harmonics coincide with a natural frequency of the stator [5]. The net forces due to the power electronics harmonic components result in significant noise.

C. Various Types of Noise

There are various types of noise that, based on their properties, have different effects on the acquired signal. It is possible to discriminate the signal from the noise based on the frequency components. The signal may contain mostly low-frequency components while the noise may spread out over the wide frequency range or the noise may only contain high-frequency components. Noise is characterized based on its frequency spectrum, which is commonly described in terms of noise color. The noise is categorized as white noise, pink noise, Brownian noise, blue noise, violet noise, and grey noise. Each noise type is specified according to the frequency distribution of its power spectral density.

1. White noise is a random noise that has equal power over the entire frequency range.
2. Pink noise is characterized by high power at low frequencies.
3. Brownian noise's amplitude is proportional to the square of the frequency over a frequency range.
4. Blue noise has strong power at high frequency and is not common in experimental measurement.
5. Violet noise, which is a differentiation of white noise, has a power spectral density that is proportional to the square of the frequency over the finite range.

III. Gray noise is a random white noise with an inverted A-weighting curve. The Experimental Set-up

A custom-made 100 *kVA*, 400 *V*, 14 poles salient pole synchronous generator is used to investigate the effect of noise on acquired signals under short circuit fault (Fig. 1). A 90 *kW*, 4 pole induction motor is utilized to drive the coupled synchronous generator. The shaft of the rotor is connected to the generator by using a gearbox. A programmable converter is used to feed the induction motor. The field winding of the generator is supplied by a DC power supply. A Hall-effect sensor (AST244) with a ratio of induced voltage to the magnetic field equal to 2.54 *T/V* is installed inside the air gap to acquire the air gap magnetic field. The datasheet specifies that the sensor should be supplied by a 2 *mA* DC current source. However, due to considerable electromagnetic interference, the magnitude of the current power supply is increased to 4-*mA* to increase the signal-to-noise ratio. A high-resolution (16-bit) oscilloscope is used to sample the
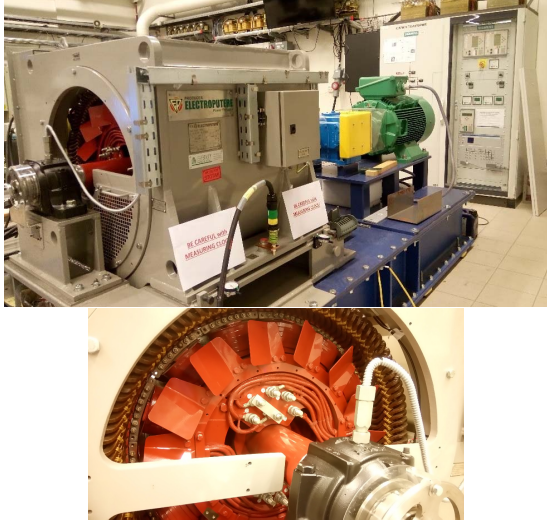
Fig. 1. The laboratory set-up of a 100 kVA salient pole synchronous generator (top), the inter-turn short circuit fault applied in the rotor.

data at 10 *kHz*. A copper shunt is used to make inter-turn short circuit fault on one of the rotor field winding as shown in Fig. 1.

IV. SIGNAL PROCESSING

Signal processing is a core part of the fault detection procedure. Although the extracted signals from the electrical machines, whether in a healthy or faulty mode, contain useful data, they must be analyzed using signal processing tools. The signal processing tools are categorized into three domains as below:

1. Time-domain
2. Frequency domain
3. Time-Frequency domain

There are several methods based on time, frequency, and time-frequency domains. In this paper, the gyration radius which is based on time series data mining is used as a time-domain processor. The fast Fourier transform (FFT) which is a frequency domain processor is utilized to obtain frequency spectrum density of the signal. There is a wide range of time-frequency processors that are limited in this paper to short-time Fourier transform (STFT), discrete wavelet transforms (DWT), and continuous wavelet transforms (CWT).

A. Noise Recognition in Measured Data

The air gap magnetic field is measured by using a Hall-effect sensor installed on the stator tooth as seen in Fig. 2 (a). The air gap magnetic field is vulnerable to a combination of the internal and external sources of noise. The internal electromagnetic noise is due to the machine configuration which leaks into data. The external noise that leaks into the acquired signal has occurred during data acquisition or storage process. Fig. 3 represents the acquired air gap magnetic field in the presence of noise.

The acquired signal is analyzed to recognize the type of noise that leaked into that. According to the definitions provided in section II-C, the behavior of the obtained signal by a sensor resembles white Gaussian noise.
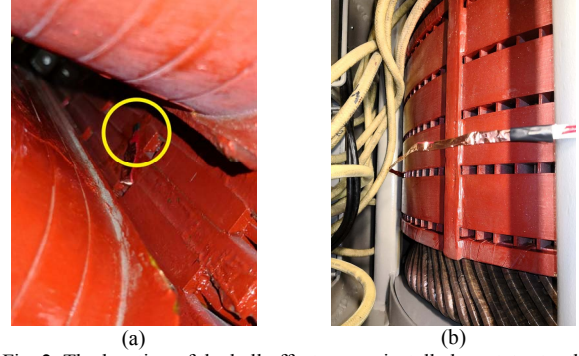

Fig. 2. The location of the hall-effect sensor installed on stator tooth (a), the shielded wire of sensor getting out of stator core to the oscilloscope (b).
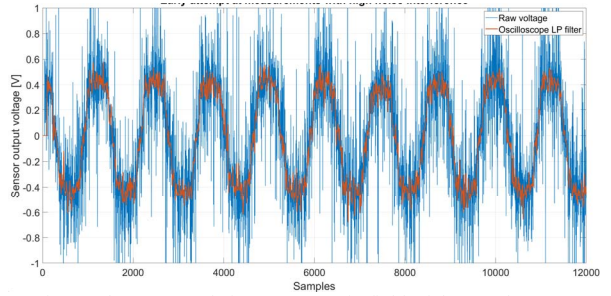

Fig. 3. The measured air gap magnetic field of the synchronous generator in the laboratory.

Since the signal is vulnerable to the noise, a specific copper shield is used to protect the sensor wires all the way to the DC power supply as shown in Fig. 2 (b). The connection between the DC power supply to the oscilloscope is made by using coaxial cable. Moreover, there are some low pass filters designed inside the oscilloscope that may help to reject or reduce the noise effect as depicted in Fig. 3.

B. Fast Fourier Transform

The distorted magnetic field caused by inter-turn short circuit (ITSC) fault contain sub-harmonics that can be distinguished based on the index as below:

$$f_{sub-harmonics} = (p \pm k)\frac{f_s}{p} \tag{1}$$

where f_s is stator terminal frequency, p is the number of poles, and k is an integer. Fig. 4 (a). depicts the spectrum density of the air gap magnetic field in healthy and under 10 short-circuited turns obtained by the FFT processor. By increasing the number of shorted turns in the rotor field winding, the amplitude of the sideband component increased. For instance, the amplitude of the sidebands for a 10 ITSC fault at frequency 7.15 *Hz*, 14.3 *Hz,* 28.6 *Hz*, and 35.7 *Hz* increased from -44.6 *dB*, -53.1 *dB*, -51.3 *dB*, and 54.9 *dB* to -36.6 *dB*, -38.9 *dB*, -39.4 *dB*, and -40.8 *dB,* respectively. Fig. 4 (b). demonstrates the effect of 20 *dB* white noise on the spectrum density of the air gap magnetic field.

The noise level of the frequency spectrum is increased from -100 dB to -50 dB by decreasing the signal-to-noise
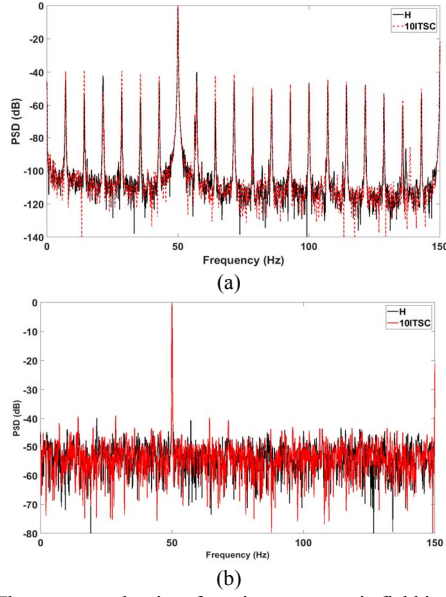
Fig. 4. The spectrum density of an air gap magnetic field in a healthy and under a 10 ITSC fault, a) without noise interference, b) with 20 *dB* SNR.

Fig. 5. The applied STFT to an air gap magnetic field in healthy (a) and under a 10 ITSC fault (b) in no-noise, 40 *dB*, and 20 *dB* SNR.

TABLE I
THE EFFECT OF VARIOUS SIGNAL-TO-NOISE RATIO ON THE NOMINATED INDEX UNDER ITSC FAULT.

		7.15 Hz	14.3 Hz	28.6 Hz	35.7 Hz	64.3 Hz	78.6 Hz
	NN	-44.6	-53.1	-51.3	-54.9	-57.4	-54.5
	60-*dB*	-44.6	-52.9	-51.2	-55.0	-57.6	-54.4
H	50-*dB*	-44.8	-53.1	-51.4	-54.1	-57.8	-54.4
	40-*dB*	-45.1	-53.0	-51.1	-55.3	-58.2	-54.4
	30-*dB*	-45.3	-55.1	-51.5	-54.8	-57.3	-54.6
	NN	-39.6	-38.9	-39.4	-40.8	-41.8	-49.3
	60-*dB*	-39.6	-38.9	-39.4	-40.8	-41.8	-49.3
F	50-*dB*	-39.5	-38.9	-39.4	-40.9	-41.9	-49.5
	40-*dB*	-39.8	-39.1	-39.2	-40.6	-42.1	-49.5
	30-*dB*	-40.3	-39.1	-39.9	-40.2	-41.8	-49.1

Fig. 6. The impact of 40 *dB* noise on processed data by STFT (a), and the impact of a 10 ITSC fault on a processed signal by STFT (b) by using the image processing tool.

ratio. Therefore, the magnitude of the introduced index for ITSC detection is simply masked in the case of high-level noise interference. Hence, the ITSC diagnosis under the 20 *dB* signal-to-noise ratio is almost impossible.

Table I presents the effect of various signal-to-noise ratios on the nominated index under ITSC fault. The amplitude of the index for a low degree of SNR is acceptable which is in the range of internal noise. However, the signal-to-noise ratio of 20 dB is the borderline of accurate fault detection. By decreasing the SNR, the amplitude of sidebands even in a healthy case is masked and it may lead to false alarm of the fault indication.

C. Short-Time Fourier Transform

Fig. 5. presents the applied short-time Fourier transform (STFT) to the measured air gap magnetic field in a healthy and a 10 ITSC fault with different amounts of white additive Gaussian noise. The STFT is performed with a window length of one electric period. Introducing an index based on the processed signal by using STFT is not in the scope of this paper. However, a comparison between the healthy and faulty STFT reveals that the fault has a significant impact on two bands of STFT
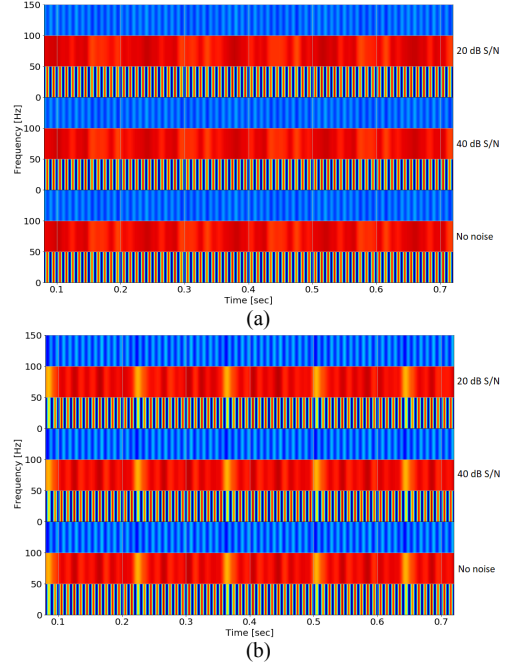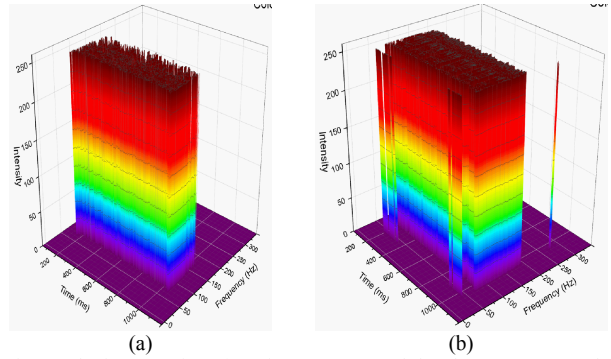
between 0 to 100 *Hz*.

A qualitative comparison of the healthy and faulty signal by the introduction of noise implies that noise does not mask the frequency bands to a great extent which is likely due to the long window length. However, a qualitative comparison is not reliable for fault detection. A healthy signal with 40 *dB* noise and a 10 ITSC faulty signal without noise which are processed by STFT is fed to the image processing tool as shown in Fig. 6. As seen in Fig. 6 (a), the noise has the same pattern as ITSC fault with sparse frequency components. Therefore, noise with a higher ratio may lead to false fault identification. A caveat of STFT analysis in the presence of noise is that increasing the window length to reject noise will reduce the temporal resolution and limit its usefulness.

D. Continuous Wavelet Transform

The continuous wavelet transforms (CWT) is a qualitative signal processing tool which is used in fault detection of the electric machines. The CWT is performed using the frequency B-spline wavelet.
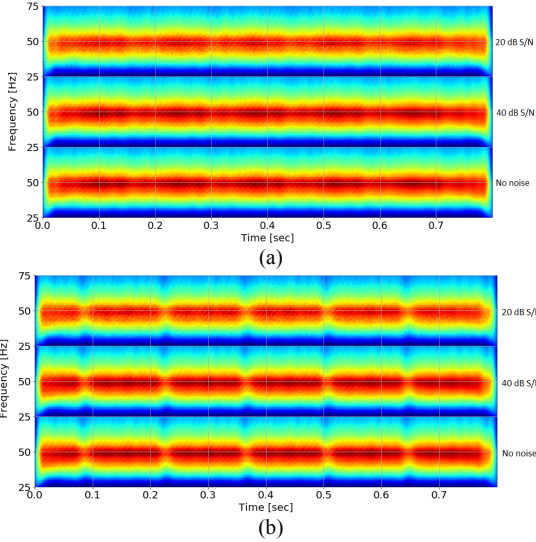
Fig. 7. The applied CWT to an air gap magnetic field in healthy (a) and under a 10 ITSC fault (b) in no-noise, 40 *dB*, and 20 *dB* SNR.

The data interpretation of the processed signal by CWT is arduous since it must be analyzed by a convolutional neural network or image processing expert. Fig. 7. depicts the applied CWT to a measured air gap magnetic field of a healthy and faulty machine. A comparison between the healthy and a 10 ITSC fault between the frequency bands of 25 *Hz* to 75 *Hz* indicates that fault presence changes the CWT profile by introducing a periodic notch.

The effect of white Gaussian noise on CWT is studied by adding different amounts of noise. The intensity of the CWT is reduced by increasing the noise level. Moreover, the notching of the 50 *Hz* band, is severely weakened by the introduction of noise. The CWT is affected uniformly across frequencies, unlike the STFT, due to its greater time-frequency resolution. The effect will vary among wavelets. Some of the noise rejecting qualities of STFT could be achieved in CWT by selecting wavelets with a greater number of oscillations, such as the Shannon mother wavelet.

E. Discrete Wavelet Transform

The discrete wavelet transform is a useful signal processing tool for feature extraction of the electric machine under a faulty condition. The DWT is commonly implemented based on filter banks. Each level of the filter consists of a low-pass filter and high-pass filter which the output is downsampled by factor 2 at each level. The output of the high-pass filter is known as a detailed signal while the output of the low-pass filter is called an approximate signal. The decomposed signal by DWT depends on the type of mother wavelet. In this paper, Daubechies 8 is used to decompose the air gap magnetic field into various frequency sub-bands. Since the sampling frequency is 10 kHz, the first, and second detailed sub-band is between 5000-2500 *Hz*, and 2500-1250 *Hz*, respectively.

The energy of each sub-bands level is introduced as a proper signature to diagnose the occurrence of the ITSC fault. The energy of the signal is as below:

TABLE II
THE ENERGY OF VARIOUS WAVELET SUB-BANDS ENERGY IN HEALTHY AND A 10 ITSC FAULT. (NL: NOILSELESS) (NI: NOISE INCLUDED)

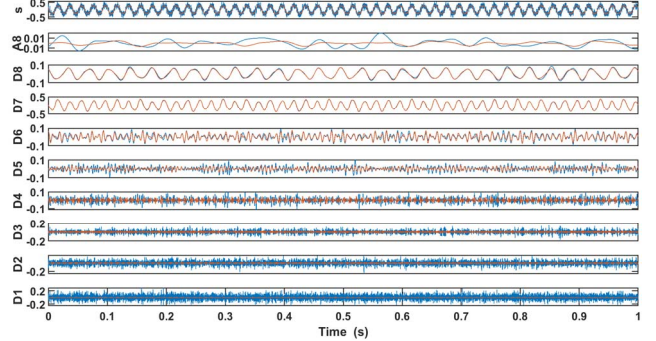| Energy	D8	D7	D6	D5	D4	D3	D2	D1
H-NL	0.70	0.38	0.83	0.94	0.97	1	1.06	1.35
F-NL	0.70	0.38	0.81	0.88	0.83	0.79	0.72	0.65
H-NI	0.70	0.38	0.81	0.88	0.83	0.79	0.72	0.65

Fig. 8. The discrete wavelet transforms of air gap magnetic field in a healthy case (red), and with 20 *dB* white gaussian noise (blue).

$$E = \int_{-\infty}^{+\infty} |D_n|^2 \, dt \qquad (2)$$

where D_n is the magnitude of each DWT sub-bands. The occurrence of 10 ITSC faults in one rotor pole leads to an increment of the energy of D1 to D6 as shown in Table. II. Therefore, by comparing the energy variation of the different wavelet sub-bands in a healthy and faulty case, the occurrence and progression of fault are discernible.

Fig. 8 shows the discrete wavelet transforms of the air gap magnetic field in a healthy case without noise effect and under a noisy condition with a signal-to-noise ratio of 20 *dB*. Although noise has significant impacts on detailed sub-bands especially D1 to D6, it also affects the amplitude of the D7, D8, and A8. However, the energy of wavelet sub-bands of the healthy machine with 20 *dB* white Gaussian noise is equal to the energy level of corresponding wavelet sub-bands under a 10 ITSC faults. For instance, the amplitude of the energy of sub-bands of D3, D2, and D1 for the healthy machine in a noisy environment are decreased to 0.79, 0.72, and 0.65 while the energy of the same sub-bands for a 10 ITSC fault is also the same. Consequently, the noisy environment leads to a false alarm that significantly affect the fault detection.

F. Time Series Data Mining

The inter-turn short circuit fault of the rotor results in a non-uniform magnetic field. The radius of gyration (RG) which is based on time series data mining (TSDM) approach can represent the variation rate of the faulty signal. If a trend of time variation of the signal is high, its average value for the different operating points may be utilized to extract the suitable index based on RG. For a given time series of the magnetic field of air gap as below:

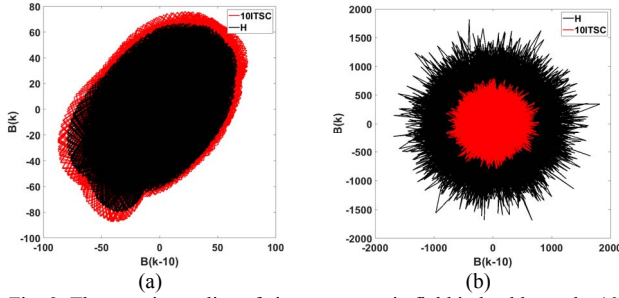$$B = \{B(k) - B(k-1), \quad k = 2,3,...,j\} \qquad (3)$$

Fig. 9. The gyration radius of air gap magnetic field in healthy and a 10 ITSC faults without noise (a) and with 20-dB white gaussian noise (b).

where j is the number of the sampled signal, and k is the time index. Reconstructed phase space for k equal to 10 is shown in Fig. 9 (a). A TDSM is used to generate the mass based on variation in the magnetic field time series. The RG is applied to the generated mass to quantify the rate of changes as below:

$$RG = \sqrt{\left(\frac{\sum_{k=1+l}^{j} \left((B(k-\mu_0)^2 + (B(k-l)-\mu_l)^2 \right)}{j-l} \right)} \qquad (4)$$

where μ_0 and μ_1 are the center of gyration, and l is the time lag of the phase space. The applied RG to magnetic flux density in healthy and under a 10 ITSC fault is 61 and 78 respectively. As shown in Fig. 9 (a), the fault leads to distortion of the magnetic field which results in increment in the radius of mass.

Fig. 9 (b) represents the applied TSDM to the healthy and faulty air gap magnetic field in a presence of 20 dB white Gaussian noise. The magnitude of the RG is considerably increased in comparison to the noiseless signal. Moreover, the area of the mass and correspondingly the radius of the gyration in healthy cases is enormously larger than the faulty case. Therefore, the input signal to the TSDM algorithm must be noiseless otherwise it leads into inaccurate fault signature.

V. CONCLUSIONS

This paper discussed thoroughly the various kinds of noise that may exist in the industrial environment and demonstrated how it can negatively affect the measured data. A detailed investigation on the frequency component of the measured noisy data revealed that it contains the white Gaussian noise, which is the most prevalent type of noise in power industries.

The air gap magnetic field of a 100 kVA salient pole synchronous generator in healthy and under inter-turn short circuit fault is measured. The acquired signal is susceptible to a high level of noise inside the machine, which could be rejected by using specific copper shielding. In addition, the signal-to-noise ratio of the measured air gap magnetic field is increased by increasing the magnitude of the current feeding into the sensor. Furthermore, it is necessary to use coaxial cable to avoid any noise leakage into the sensor from outside the machine.

Signal processing tools are the key point of the fault detection procedure of the electric machines. Based on the level of leaked noise into the signal, the processed data may indicate a false result. However, the detection of the fault in a noisy condition depends on the proposed feature. The sensitivity of the indices and signal processing tools under noisy condition summarized as:

1. FFT: It is only sensitive to high-level noise and sidebands are masked with 20 dB noise.
2. STFT: It is sensitivity to noise and resolution of the frequency bands depend on the length of the window.
3. CWT: It is highly sensitive to noise and may lead to a false alarm.
4. DWT: It depends on frequency sub-band which is utilized for feature extraction.
5. TDSM: It is highly sensitive to noisy data.

REFERENCES

[1] I. Sadeghi, H. Ehya, J. Faiz, and A. A. S. Akmal, "Online condition monitoring of large synchronous generator under short circuit fault — A review," *2018 IEEE International Conference on Industrial Technology (ICIT), Lyon*, 2018, pp. 1843-1848.

[2] B. M. Ebrahimi, J. Faiz and M. J. Roshtkhari, "Static-, Dynamic-, and Mixed-Eccentricity Fault Diagnoses in Permanent-Magnet Synchronous Motors*," IEEE Transactions on Industrial Electronics*, vol. 56, no. 11, pp. 4727-4739, Nov. 2009.

[3] P. Vijayraghavan and R. Krishnan, "Noise in electric machines: a review," *Conference Record of 1998 IEEE Industry Applications Conference. Thirty-Third IAS Annual Meeting (Cat. No.98CH36242)*, St. Louis, MO, USA, 1998, pp. 251-258 vol.1.

[4] R. S. Girgis, M. Bernesjo, and J. Anger, "Comprehensive analysis of load noise of power transformers," *2009 IEEE Power & Energy Society General Meeting*, Calgary, AB, 2009, pp. 1-7.

[5] Yang, S. J. "Effects of voltage/current harmonics on noise emission from induction motors." *Vibrations and Audible Noise in Alternating Current Machines. Springer, Dordrecht*, 1988. 457-468.

[6] H. Tischmacher, I. P. Tsoumas, B. Eichinger, and U. Werner, "Case Studies of Acoustic Noise Emission From Inverter-Fed Asynchronous Machines," in *IEEE Transactions on Industry Applications*, vol. 47, no. 5, pp. 2013-2022, Sept.-Oct. 2011.

[7] I. P. Tsoumas and H. Tischmacher, "Influence of the Inverter's Modulation Technique on the Audible Noise of Electric Motors," *IEEE Transactions on Industry Applications*, vol. 50, no. 1, pp. 269-278, Jan.-Feb. 2014.

[8] J. Qin, P. Sun and J. Walker, "Measurement of field complex noise using a novel acoustic detection system," *2014 IEEE AUTOTEST*, St. Louis, MO, 2014, pp. 177-182.

[9] S. M. J. Ali, "Measurement of vibration and noise level at power plant and refinery companies that represents a condition monitory for the health of machines," *2017 International Conference on Environmental Impacts of the Oil and Gas Industries: Kurdistan Region of Iraq as a Case Study (EIOGI)*, Koya-Erbil, 2017, pp. 85-87.

[10] D. P. Martins and M. S. Alencar, "A new approach to noise measurement and analysis in an industrial facility," *2014 IEEE International Instrumentation and Measurement Technology Conference (I2MTC) Proceedings*, Montevideo, 2014, pp. 964-967.